Recent Developments in Meshless and Extended Finite Element Methods

T. Belytschko[a] , J. X. Xu[a] , J. Chessa[a] , N. Moes[b] , A. Gravouil[c]

a. Department of Mechanical Engineering, Northwestern University Evanston IL. USA 60248-3111
b. Laboratoire de Mėcanique et Matėriaux, Ecole Centrale de Nantes, 1 Rue de la Noe, 44321 Nantes, FRANCE
c. Laboratoire de Mėcanique de Solides, Institut National des Sciences Appliquėes de Lyon, 34 Av. Des Arts, 69621 Villeurbanne, FRANCE

Abstract

Methods based on the partition of unity for approximating discontinuous function in finite element and meshless formulations and described. In finite element methods, they enable solutions with discontinuities that are independent of the mesh to be created. Therefore evolving discontinuities require no remeshing. In meshless methods, the schemes provide greater accuracy and versatility than techniques based on the visibility criterion. Solutions for several examples are presented.

1 Introduction

This paper discusses the approximation of functions with arbitrary discontinuities and discontinuous derivatives by meshless methods and the extended finite element method (XFEM). In the extended finite element method, the discontinuities are completely independent of the finite element mesh: they can cross elements in any manner. This is particularly useful for evolution problems with moving discontinuities, such as solidification, phase changes, cracks, shear bands and joints in rock. In problems involving the evolution and motion of discontinuities, meshless methods and XFEM avoid the need for remeshing as the discontinuities evolve. These methods provide a powerful tool for modeling problems in engineering, such as bolts, jointed rock, sleeves, bubbles, etc. In these problems, it avoids the need for sliding interfaces that conform to the mating meshes.

The techniques for approximating discontinuities are based on the concepts described in Belytschko and Black (1999), Moes et al (1999), Dolbow et al (2001) and Belytschko et al (2001). We emphasize modeling in finite element methods, but these methods also apply to meshfree approximations such as the element-free Galerkin method EFG, Belytschko, Lu and Gu (1994). Other papers which address the issue of discontinuous elements are Oliver et al (1995), Duarte et al

(2001) and Rashid (1998). The methods proposed here differ from the first two in that there are no incompatibilities in the element and smooth surfaces of discontinuity can be constructed. The method of Duarte et al (2001) also introduces no discontinuities in the function, and provides an alternative method for discontinuous functions based on the visibility criterion.

In the discontinuous approximations described here, the surfaces of discontinuity are defined by signed distance functions. This is not necessary for the application of these discontinuous approximations, but they are very appealing because the methodology of level sets can then be applied to update these surfaces, Osher and Sethian(1998). Other workers who have proposed level sets for finite elements are Rao et al. (2000), Stolarska et al. (2001) and Sukumar et al. (2001). Related work is the generalized FEM, Stroubolis et al (2000).

The major appeal of these methods for incorporating discontinuities in finite elements is that they do not require the mesh to conform to discontinuities in the approximating function or its derivatives. They also avoid remeshing for moving discontinuities. Meshing, particularly with triangles and tetrahedra, has achieved a high level of robustness and speed, and many are tempted to use it for everything. It is our belief that in many cases, methods that avoid remeshing are preferable, for the costs of remeshing lie not only in the cost of creating a new mesh, but the tremendous overhead associated with adapting visualization techniques and other post-processing features, such as time histories past selected points, to sequences of meshes in evolution problems.

2 Approximations for Discontinuities

2.1 Discontinuities in Functions

We consider a domain Ω with boundary Γ as shown in Figure 1. We first describe the method for the approximation of a scalar variable $u(\mathbf{x})$, but the method is easily extended to vector.

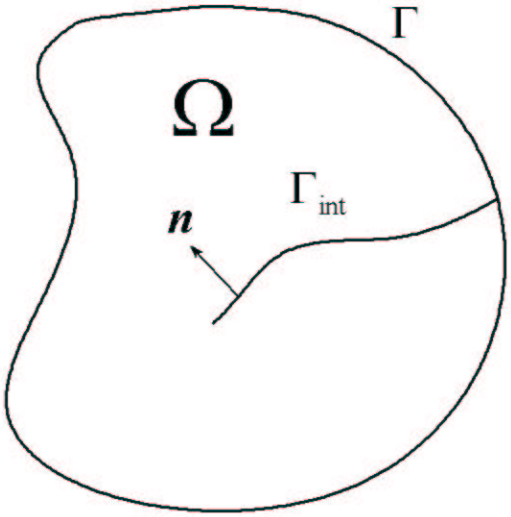


Figure 1. Nomenclature for discontinuity

For the construction of an approximation with a discontinuity on Γ_{int}, we use mesh that is completely independent of the geometry or location of the discontinuity. The mesh consists of n_e elements and n_n nodes. We denote the shape functions at node I by $N_I(\mathbf{x})$ and the corresponding nodal values of the dependent variable by u_I. All of the discrete approximations are of the following form

$$u(\mathbf{x}) = \sum_I N_I(\mathbf{x})\big(u_I + a_I \phi_I(\mathbf{x})\big) \tag{1}$$

where u_I are nodal values and a_I are additional degrees of freedom associated with the enrichment $\phi_I(\mathbf{x})$ for the discontinuity.

Although the surfaces can be represented by any technique, for convenience we describe the surfaces of discontinuity Γ_α by signed distance functions $f_\alpha(\mathbf{x})$. The signed distance function is defined by

$$f_\alpha(\mathbf{x}) = \min_{\bar{\mathbf{x}} \in \Gamma_\alpha} \|\mathbf{x} - \bar{\mathbf{x}}\| \, sign\Big(\mathbf{n}^+ \cdot (\bar{\mathbf{x}} - \mathbf{x})\Big) \tag{2}$$

where $\bar{\mathbf{x}}$ is a point on the surface of discontinuity Γ_{int} and $\mathbf{n}^+$ is a unit normal to the surface of discontinuity from the subdomain where the distance function is positive. The $\mathbf{n}^+$ can be placed in either direction, but it always will point into the subdomain where the distance function is negative. As is well known, the point $\bar{\mathbf{x}}$ is the closest point projection of $\mathbf{x}$ on Γ_α, which is the orthogonal projection for a smooth surface; see Figure 1 for a depiction of the ingredients of the above equation at a typical point. In most of the following we represent the distance function by the finite element or meshless approximation

$$f_\alpha(\mathbf{x}) = \sum_I f_{\alpha I} N_I(\mathbf{x}) \tag{3}$$

where $N_I(\mathbf{x})$ are the shape functions. When $N_I(\mathbf{x})$ are the standard C^0 finite element shape functions for continua, the surface (or line in 2D) of discontinuity is C^0, i.e. piecewise continuously differentiable. If smoother representations of the surface are desired, moving least square approximations such as those described for meshless methods in Belytschko, Liu and Gu (1994) can be used, even when the solution approximation is based on finite elements.

The structure of the approximation depends on whether the support of $N_I(\mathbf{x})$ (i.e. the domain on which $N_I(\mathbf{x})$ is nonzero) is bisected (i.e. cut completely in two) by the discontinuity or whether the discontinuity ends within the support of $N_I(\mathbf{x})$. The two cases are illustrated in Fig. 2. The support of $N_I(\mathbf{x})$ generally includes the domains of all elements which share node I. When any element in the support of $N_I(\mathbf{x})$ is bisected by the discontinuity, we call it a bisected support. If the discontinuity only partially cuts the support, we call it a slit support.

On a bisected support, the enrichment for representing a discontinuity in the function is given by

$$\phi_I(\mathbf{x}) = \overline{H}\left(f_\alpha(\mathbf{x})\right) \tag{4}$$

where

$$\overline{H}(\mathbf{x}) = H(\mathbf{x}) - H\left(\mathbf{x}_I\right) \tag{5}$$

and $H(\mathbf{x})$ is a step function given by

$$H(\mathbf{x}) = \begin{cases} 0 \ \ for\ \mathbf{x} < 0 \\ +1 \ for\ \mathbf{x} > 0 \end{cases} \tag{6}$$

Inserting into (1) we can see that the approximation at an enriched node is

$$\psi_I\left(\mathbf{x}, u_I, a_I\right) = N_I(\mathbf{x})\left(u_I + a_I H\left(f_\alpha(\mathbf{x})\right)\right) \tag{7}$$

The above can be viewed as an enrichment of the element with a windowed step function, where $N_I(\mathbf{x})$ is the window function. The window function localizes the enrichment so that the discrete equations will be sparse. The degrees-of-freedom a_I are associated with the enrichment. It is also an example of a partition of unity, Melenck and Babuska (1996), since the functions $N_I(\mathbf{x})$ form a partition of unity.

In earlier work we used

$$\psi_I\left(\mathbf{x}, u_I, a_I\right) = N_I(\mathbf{x})\left(u_I + a_I H\left(f_\alpha(\mathbf{x})\right)\right) \tag{8}$$

which is in many senses equivalent to (3). By replacing $f(\mathbf{x})$ by $f(\mathbf{x}) - f\left(\mathbf{x}_I\right)$, the portion of the enrichment functions that represented by $N_I(x)$ are dropped. This modification is not essential but helps in the physical interpretation of the degrees of freedom and it reduces the number of elements which are modified by the enrichment. In the above, the enrichment introduces the step function along the curve $f_\alpha(\mathbf{x}) = 0$. The coefficients a_I will be additional unknowns in the discrete equations and govern the magnitude of the discontinuity in the domain of the support of the shape function $N_I(\mathbf{x})$. This is illustrated for a one dimensional problem below.

For a slit support, the enrichment is given by

$$\psi_I\left(\mathbf{x}, u_I, a_I\right) = N_I(\mathbf{x})\left(u_I + a_{I\beta}\overline{b}_\beta(\mathbf{x})\right) \tag{9}$$

where $\overline{b}_{\beta I}(\mathbf{x}) = b_\beta(\mathbf{x}) - b_\beta\left(\mathbf{x}_I\right)$ and $b_\beta(\mathbf{x})$ are branch functions around the discontinuity. The branch functions are constructed in terms of the geometry of the surface of the discontinuity. Consider for example the discontinuity shown in Figure 2. The surface of discontinuity is extended by a tangent plane

$$\nabla f_\alpha \cdot \left(\mathbf{x} - \mathbf{x}_A\right) = 0 \tag{10}$$

The branch function is then constructed in terms of the angle θ of the local cylindrical coordinate system at the end point of the discontinuity. Generally more than one branch function is needed for each enriched node. For example, the enrichment functions can be

$$b_l(\mathbf{x}) = \left[r\, sin\frac{\theta}{2}, r^2\, sin\frac{\theta}{2} \right] \tag{11}$$

The branch function is discontinuous across the line Γ_α and is continuous and well behaved in the domain surrounding the discontinuity. For linear fracture mechanics, the branch functions

$$b_l(\mathbf{x}) = \left[\sqrt{r}\, sin\frac{\theta}{2}, \sqrt{r}\, sin\frac{\theta}{2} sin\theta, \sqrt{r}\, cos\frac{\theta}{2}, \sqrt{r}\, cos\frac{\theta}{2} sin\theta \right] \tag{12}$$

have been used in Belytschko and Black (1999). Only the first of the above functions is a branch functions; the others were added to improve the accuracy in elastic fracture problems. For the same reason, the enrichment was chosen to vary with $\sqrt{r}$. The above functions span the near-tip asymptotic solution for a crack, so very good accuracy can be obtained for these problems.

The branch function can be constructed in terms of the distance function so that it conforms to a discontinuity that is not rectilinear away from its end. The angle θ for any point $\mathbf{x}$ is defined by

$$\theta(\mathbf{x}) = tan^{-1}\left(\frac{f(\mathbf{x})}{r} \right) \tag{13}$$

This construction enables the discontinuity to be curved or piecewise linear behind the, since by defining the angle in terms of $f(\mathbf{x})$ the line of discontinuity always corresponds to $f(\mathbf{x}) = 0$.

For nodes whose supports are cut by two or more discontinuities, the enrichment must include additional functions as shown in Daux et al (2000). Consider for example the case of two discontinuities which intersect in as support as shown in Figure 6a. The approximation for the discontinuity is then given by

$$\phi_I(\mathbf{x}, u_I, a_I) = N_I(\mathbf{x})\left(u_I + a_{I1}\overline{H}\left(f_1(\mathbf{x})\right) + a_{I2}\overline{H}\left(f_2(\mathbf{x})\right) + a_{I3}\overline{H}\left(f_1(\mathbf{x})\, f_2(\mathbf{x})\right)\right) \tag{14}$$

Thus we need three additional unknowns at each node in for which the support contains a discontinuity which branches into two discontinuities. These functions are linearly independent and independent of the finite element shape functions. The above form is somewhat different from Daux et al (2000), but more compact and more easily implemented.

Another important case is a branching discontinuity, such as a branching. This is a degeneration of the above case of intersecting discontinuities. The enrichment is constructed by

$$\phi_I(\mathbf{x}, u_I, a_I) = N_I(\mathbf{x})\left(u_I + a_{I1}H\left(f_1(\mathbf{x})\right) + a_{I2}H\left(f_1(\mathbf{x})\, f_2(\mathbf{x})\right)\right) \tag{15}$$

The enrichment here consists of two linearly independent. It is also possible to add enrichments to account for the singularities which occur at intersecting discontinuities in elastic materials.

2.2 <u>Discontinuities In Derivatives</u>.

Another important class of discontinuities are those in the first derivatives of the approximation. These discontinuities occur at interfaces between materials and different phases of materials, such as at austenite-martensite interface. From a general viewpoint, we can say that discontinuities in derivatives occur wherever the coefficients of the governing partial differential equation are discontinuous. These discontinuities can easily be handled by standard finite element approximations by aligning the element edges with the discontinuity. However, if the discontinuity moves with time, remeshing is required. The approximation given below can model discontinuities in the derivatives on surfaces or (lines in two dimensions) which are independent of the mesh.

An approximation with a discontinuity in the derivative is constructed by letting the nodal approximation for a node with a bisected support be

$$\phi_I(\mathbf{x}, u_I, a_I) = N_I(\mathbf{x})\left(u_I + a_I \bar{f}_\alpha(\mathbf{x})\right) \tag{16}$$

where

$$\bar{f}_\alpha(\mathbf{x}) = |f_\alpha(\mathbf{x})| - |f_\alpha(\mathbf{x}_I)| \tag{17}$$

where $|\bullet|$ is the standard absolute value symbol. The approximation can also be written as

$$\phi_I(\mathbf{x}, u_I, a_I) = N_I(\mathbf{x})\left(u_I + a_I\left(\|f_\alpha(\mathbf{x})\| - \|f_\alpha(\mathbf{x}_I)\|\right)\right) \tag{18}$$

The enrichment is thus the absolute value of the signed distance function. This concept was introduced in Krongauz and Belytschko(1998) and Sukumar et al(2001).

For a support which is cut by the discontinuity, the approximation is

$$\phi_I(\mathbf{x}, u_I, a_I) = N_I(\mathbf{x})\left(u_I + a_I b_{\alpha I}^D(\mathbf{x})\right) \tag{19}$$

where $b_{\alpha I}^D(\mathbf{x})$ can be selected from the following branch functions

$$b_{\alpha I}^D(\mathbf{x}) = \left[r\cos\frac{\theta}{2}, r^2\cos\frac{\theta}{2}, \sqrt{r}\cos\frac{\theta}{2}, \right] \tag{20}$$

The branch function is continuously differentiable within the domain but is cusp like across Γ^D.

For intersecting discontinuities in derivatives, the same procedure as for discontinuities in the function is used. For example, for two intersecting discontinuities, the approximation is

$$\phi_I(\mathbf{x}, u_I, a_I) = N_I(\mathbf{x})\left(u_I + a_{I1}\bar{f}_1(\mathbf{x}) + a_{I2}\bar{f}_2(\mathbf{x}) + a_{I3}\bar{f}_1(\mathbf{x})\bar{f}_2(\mathbf{x})\right) \tag{21}$$

The construction of discontinuities of a single component in a vector function, such as a shear band, is simplified by the use of the signed distance function. The unit normal to the line of discontinuity is given by

$$\mathbf{e}_n = \nabla f \tag{22}$$

The tangent plane is then defined by any two unit vectors orthogonal to $\mathbf{e}_n$, which we denote by $\mathbf{e}_1$ and $\mathbf{e}_2$. The approximation for a bisected support is then given by

$$\mathbf{u}(\mathbf{x},t)=\sum_I \left(N_I(\mathbf{x})\mathbf{u}_I(t)+a_1(t)N_I(\mathbf{x})H\left(f(\mathbf{x})\right)\mathbf{e}_1+a_2(t)N_I(\mathbf{x})H\left(f(\mathbf{x})\right)\mathbf{e}_2\right) \tag{23}$$

For a bisected support, the approximation is given by the above with the step function replaced by branch functions.

2.3 Meshless Method

The application of these techniques to meshless methods is identical to their application in finite element methods. The approximations at nodes whose support is cut by the discontinuity are given by Eq. (8), whereas the approximations at nodes that are partially slit by the discontinuity are given by Eq. (9). The domains where these two approximations apply for support of radius r are shown in Figure 2; $r=1.8h$, where h is the nodal spacing. This approach avoids the need for the visibility and transparency methods used in EFG, see Ventura et al (2002) for details.

3 Examples

3.1 Exact Solution for Mode I Crack

To illustrate the performance of this approach in meshless methods, the crack problems in Figure 1 is considered. A closed form solution for this mode I problem can be constructed by using the well-known near-tip stress field and prescribing the traction at the boundary according to this field. The rigid-body motions are suppressed by the constraints at two nodes as illustrated in Figure 2. A square patch with unit side and a crack of length 0.5 is considered. This problem is used to compare the performance of the enriched EFG against the visibility criterion.

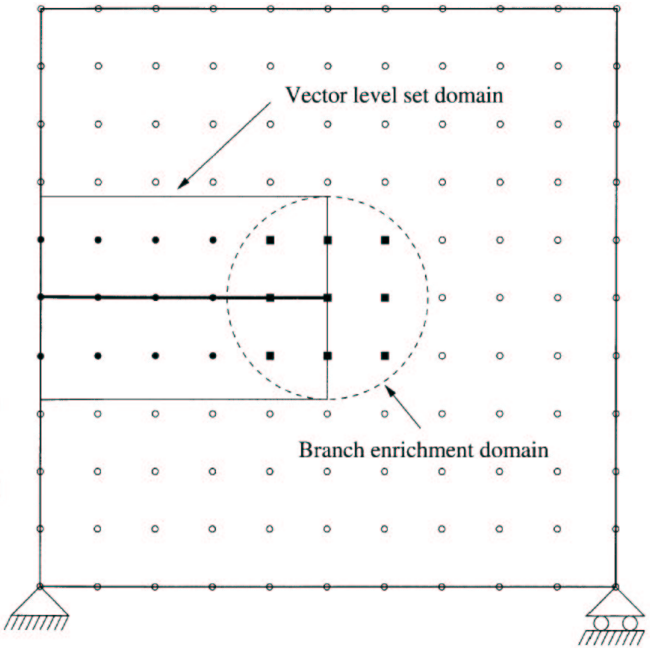


Figure 2. Discretization and enriched nodes for accuracy analysis. Filled circles and squares are jump and branch enriched nodes, respectively.

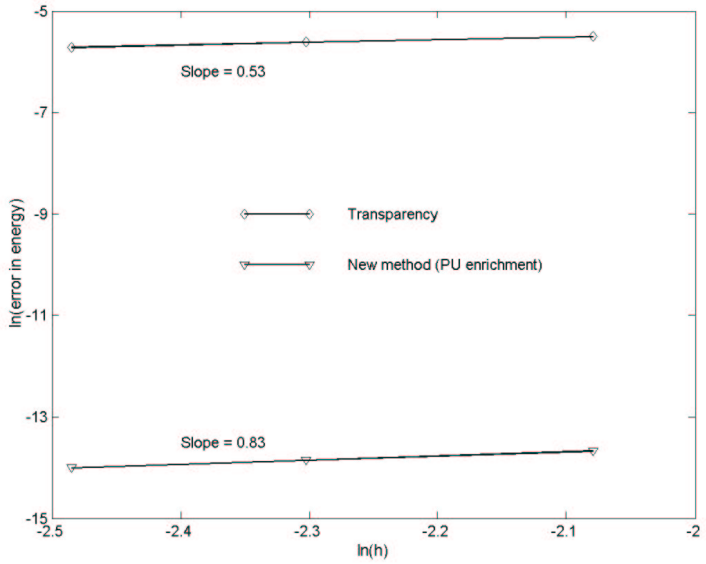


Figure 3. Logarithms of the relative error in energy vs. logarithm of the mesh size.

The stress intensity factor is prescribed as $K_1 = 1.0\ \mathrm{Nm}^{-3/2}$, and the following relative error in energy is computed:

$$\text{error in energy} = \frac{\left\| u - u^h \right\|}{\left\| u \right\|} = \frac{\left(\int_\Omega (\varepsilon - \varepsilon^h)^T C (\varepsilon - \varepsilon^h) d\Omega \right)^{1/2}}{\left(\int_\Omega \varepsilon C \varepsilon d\Omega \right)^{1/2}} \tag{24}$$

where C is the Hookean tensor. The jump function enrichment is introduced on those nodes whose supports are cut by the crack, while the branch function enrichment is considered on those nodes whose support are slit by the crack, see Fig 2. The new method greatly increase the accuracy of the approximation and the convergence rate is improved as well. These results are reported in Figure 2, where the natural logarithm of the relative error in energy is plotted as a function of the logarithm of the mesh size h, given by the spacing between the nodes.

3.2 Crack growth from a fillet by Meshless Method

This example shows the growth of a crack from a fillet in a structural member. The experiment to be modeled is shown in Fig 4, with the computational domain outlined with a dashed line. The

experiment is taken from experimental work found in (Sumi, Yang, and Wang, 1996). In this example, we investigate the effect of the thickness of the lower I-beam on crack growth. Only the limiting cases for the bottom I-beam of a rigid constraint (very thick beam) and flexible constrain (very thin beam) are considered. In addition, the residual stresses due to welding between the member and the I-beam are neglected.

The material is plane strain, linear elastic with Young's modulus and Poisson's ratio of E = 200 GPa and ν = 0.3, respectively. The applied load is P = 1.0 N and the fillet radius is ρ = 20 mm. The initial crack length is a_0 = 5 mm. To model a rigid constraint, the displacement in the vertical direction is fixed along the entire bottom of the domain. A flexible constraint is idealized by fixing the vertical displacement at both ends of the bottom of the domain. For both sets of boundary conditions, an additional degree of freedom is fixed to prevent a rigid body translation. The model is discretized with 1025 nodes, we simulate crack growth with a step size of Δa = 5 mm for a total of 14 steps. Figure 4 and Figure 5 shows the nodes in the vicinity of fillet and the crack paths for the cases of thick I-beam and a thin I-beam. The results shown are consistent with the experimental (Sumi, Yang, and Wang, 1996).

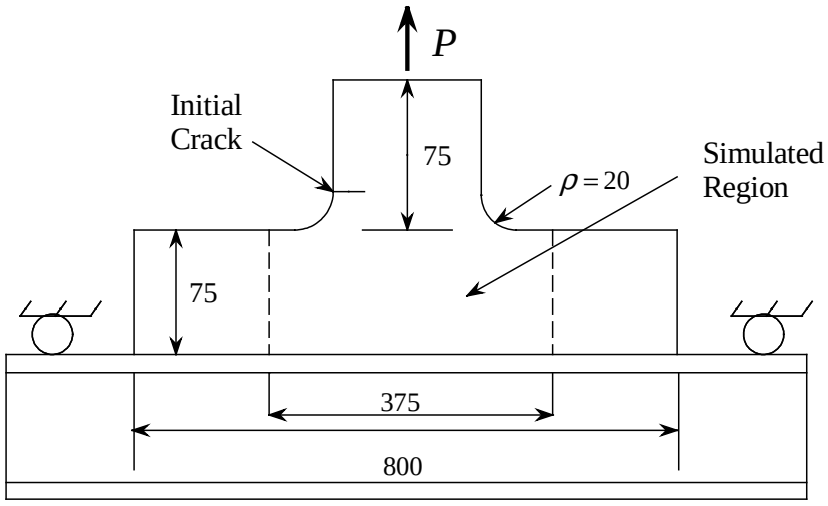
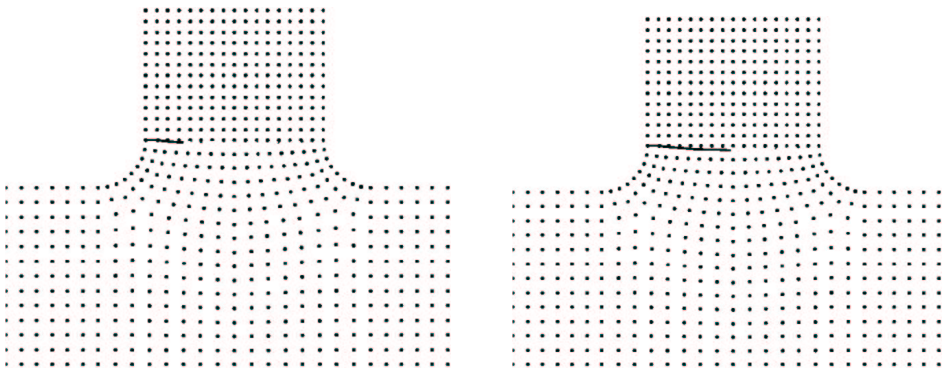


Figure 4. Experimental configuration for crack growth problem



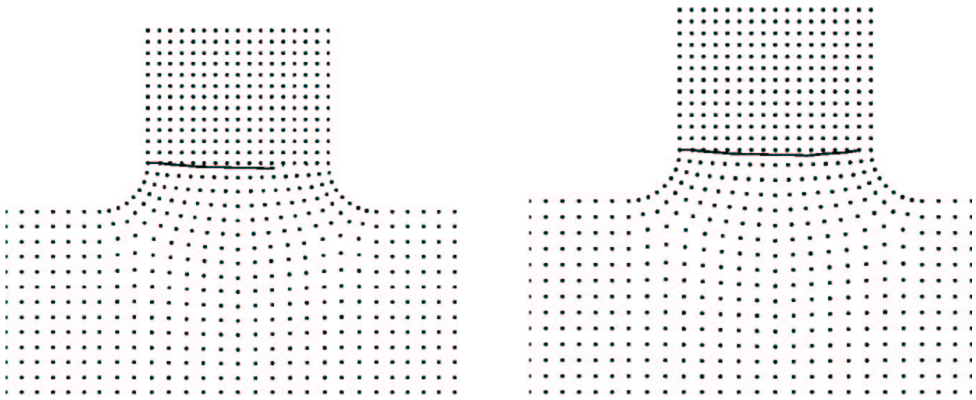


Figure 5. Crack path from a fillet for the case of a rigid I-beam.

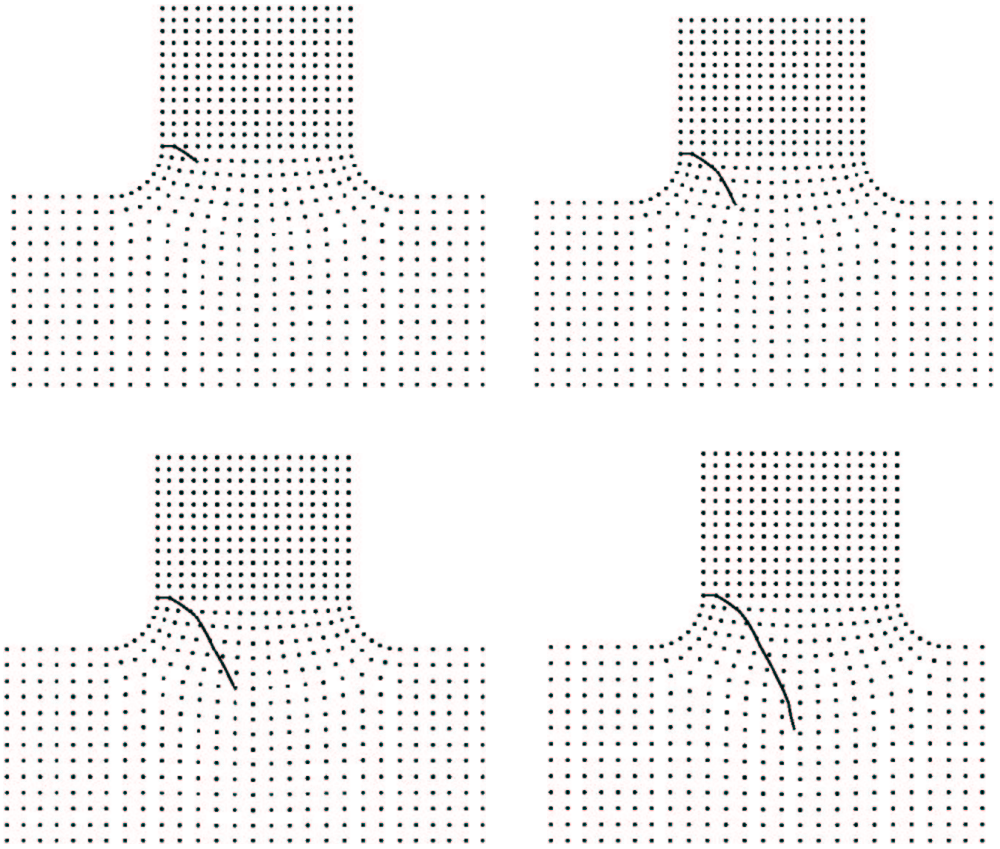


Figure 6. Crack path from a fillet for the case of a thin I-beam.

3.3 Three Dimensional Crack by XFEM

This example considers the growth of a crack in a three-dimensional beam model under bending. The extended finite element method is used, for details see Moes et al (2002) and Gravouil et al (2002). The material properties are elastic and isotropic with Young's modulus $E = 280$ GPa and Poisson's ratio $v = 0.3$. We consider fatigue crack growth governed by the Paris law, which gives the rate of crack growth in mode I in terms of load cycles N by

$$\frac{da}{dN} = CG^m$$

where *C* is a constant fit to experimental results and *G* is the maximum energy release rate. We consider the cycles *N* a time-like variable so the expression for the crack front velocity is :

$$\mathbf{V} = CG^m\left(\cos\theta_c \mathbf{n}_\psi + \sin\theta_c \mathbf{n}_\phi\right)$$

where θ_c, the angle of the velocity to the plane tangent to the crack (or $\mathbf{n}_\phi$), is obtained by:

$$\theta_c = 2\arctan\frac{1}{4}\left(\frac{K_I}{K_{II}} - sign(K_{II})\sqrt{\left(\frac{K_I}{K_{II}}\right)^2 + 8}\right)$$

Thus, the crack growth direction depends on the mode I and mode II stress intensity factors, whereas the crack speed depends on all three through the energy release rate *G*. In the numerical studies, for simplicity we chose $m = 1$ and $C = 1$.

We consider the beam shown in Figure 7 subjected to bending (see Lazarus et al., 2001 for a theoretical study of this problem). The beam dimensions are $h = 0.02m$, $l = 0.1m$ and $d = 0.01m$. The beam dimensions are $h = 0.02m$, $l = 0.1m$ and $d = 0.01m$. An initial edge crack along a plane at an angle α to the plane of the cross-section is used to initiate crack growth with $a = 0.01m$ and $\alpha = 45^\circ$ (see Figure 7). The initial geometry is discretized with a unstructured mesh of 2553 nodes and 13393 tetrahedrons. It is emphasized that the mesh does not conform to the crack geometry, and that the same mesh is used throughout the simulation. The crack is driven by a Paris fatigue law with the maximum circumferential stress hypothesis for the direction of crack propagation. From 15 to 25 points were used on the crack front to compute the velocity and the stress intensity factors. In this study, the beam is completely cut into two after 17 time steps. Figure 7 shows the evolution of the crack front. We can observe that the crack grows asymptotically towards the plane orthogonal to the axis of the beam.

Figure 8 shows the evolution of a semi-circular crack. Again, we observe that the crack grows asymptotically to plane orthogonal to the axis of the beam. Here, the crack front first grows to the lateral free surfaces, then normal to the surface. No changes are needed in the algorithm to account for these topological changes. Other crack propagation examples may be found in Gravouil et al., 2001.

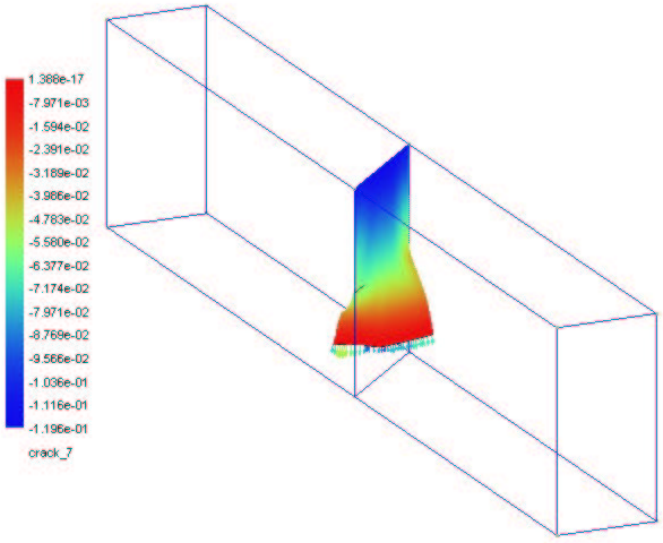
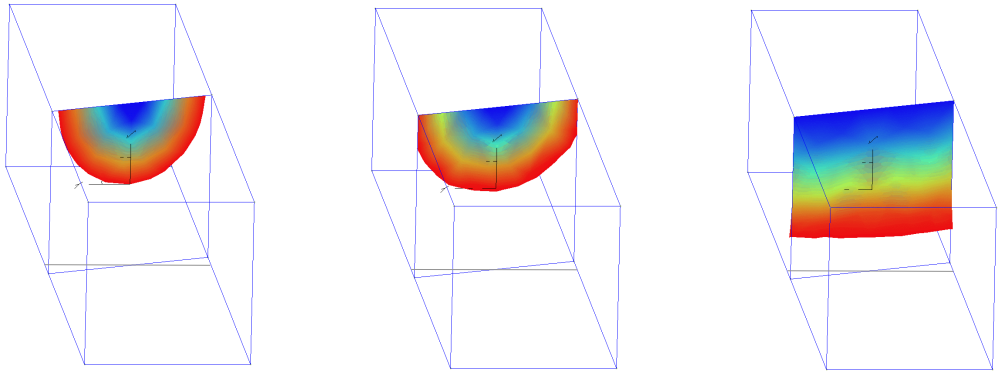


Figure 7. Crack configuration as computed by XFEM after 12 times steps



(a) (b) (c)

Figure 8. Evolution of semi-circular crack in a beam computed by XFEM

3.4 Application to Two-Phase Flow

Here we consider the application of enriched finite element approximations to the problem of two-phase flow. We consider each phase to be homogeneous and that there is no reaction or transport between the phases. For the case of no-slip at the phase interface we require the velocity field to be

continuous at the interface, but due to the differing viscosities in each phase there will be a discontinuity in velocity gradient at the interface. It is from these conditions that we use the following enriched approximations for the velocity and pressure fields are proposed.

$$v_i^h\left(\boldsymbol{x},t^n\right)=\sum_{I\in\mathcal{N}}N_I\left(\boldsymbol{x}\right)V_{iI}^n+\sum_{J\in\mathcal{N}_e}N_J\left(\boldsymbol{x}\right)\left(\left|\phi\left(\boldsymbol{x},t^n\right)\right|-\left|\phi\left(\boldsymbol{x}_J,t^n\right)\right|\right)A_{iJ}^n$$

Where $\mathcal{N}$ is the set of all nodes $\mathcal{N}_e$ is the set of enriched nodes (*i.e.* those nodes whose support is intersected by the phase interface) and $\phi\left(\boldsymbol{x},t\right)$ is a signed distance function to the phase interface. Details with respect to this application are given in Chessa et al. (2002). Figure (9) shows the results for the problem of a buoyancy driven air bubble in water which rises to, and escapes an air/water free surface interface solved. The enriched velocity approximation described above is employed. Due to the enrichment a fixed unstructured mesh is used for all time steps in the solution procedure.

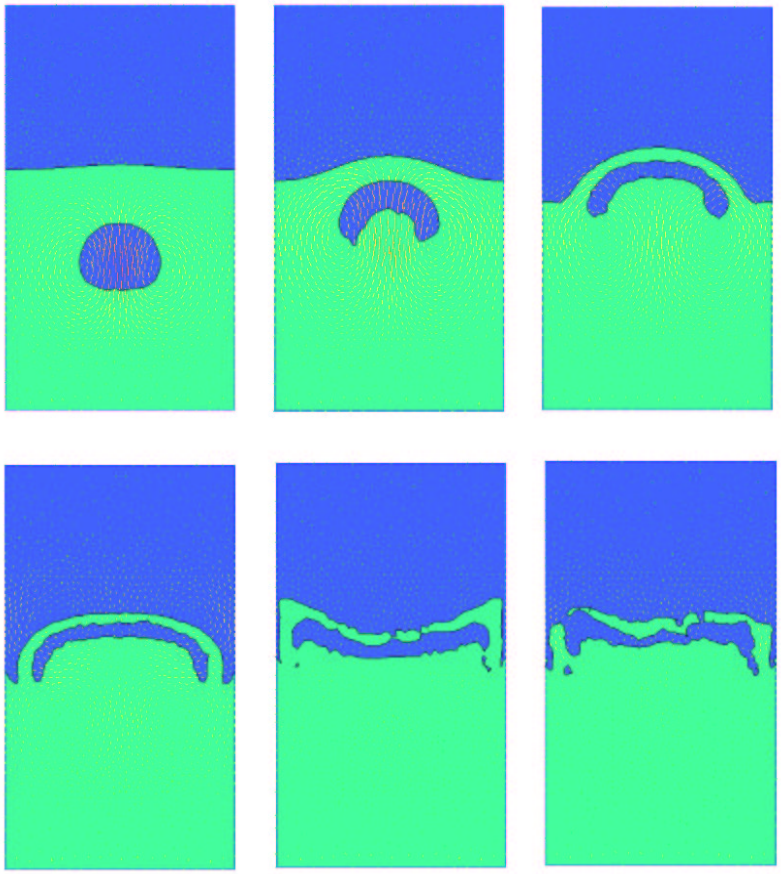


Figure 9. Plot of XFEM solution of an initially circular air bubble in water rising to an air-water free surface. The velocity field is enriched such that the rate of deformation tensor is discontinuous at all air-water interfaces. Surface tension is ignored

ACKNOWLEDGMENT

The support of the office of Naval Research is gratefully acknowledged.

REFERENCES

T. Belytschko and T. Black (1999) "Elastic Crack Growth in Finite Elements with Minimal Remeshing" International Journal for Numerical Methods in Engineering **45**(5) 601-620.

T. Belytschko, Y.Y. Lu and L. Gu (1994) "Element-free Galerkin methods" International Journal for Numerical Methods in Engineering Volume **37** 229-256.

T. Belytschko, M. Plesha and C.H. Dowding (1984) "A computer method for stability analysis of caverns in jointed rocks" International Journal for Numerical Methods in Engineering **8** 473-492.

J. Chessa and T. Belytschko (2002) "An extended finite element method for two-phase fluids" ASME Journal of Applied Mechanics *accepted for publication.*

C. Daux, N. Moës, J. Dolbow, N. Sukumar and T. Belytschko (2000)"Arbitrary branched and intersecting cracks with the eXtended Finite Element Method" International Journal for Numerical Methods in Engineering **48**(12) 1741-1760.

J. Dolbow, N. Moës and T. Belytschko (2001) "An extended finite element method for modeling crack growth with frictional contact" Computational Methods in Applied Mechanics and Engineering **190** 6825-6846.

J. Dolbow, N. Moës and T. Belytschko (2000) "Discontinuous Enrichment in Finite Elements with a Partition of Unity Method" Finite Elements in Analysis and Design **36** 235-260.

J. Dolbow, N. Moës and T. Belytschko (2000) "Modeling fracture in Mindlin-Reissner plates with the eXtended finite element method" International Journal of Solids and Structures **37** 7161-7183.

C.A. Duarte, O.N. Hamzeh, T.J. Liszka and W.W. Tworzydlo (2001) "A generalized finite element method for the simulation of three-dimensional dynamic crack propagation" Computational Methods in Applied Mechanics and Engineering **190** 2227-2262.

M. Fleming, Y.A. Chu, B. Moran and T. Belytschko (1997) "Enriched element-free Galerkin methods for crack tip fields" International Journal for Numerical Methods in Engineering **40**(8) 1483-1504.

A. Gravouil, N. Moës and T. Belytschko (2002) "Non-planar 3D crack growth by the extended finite element and level sets - Part II: Level set update" International Journal for Numerical Methods in Engineering **53**(11) 2569-2586.

Y. Krongauz and T. Belytschko (1998) "EFG approximation with discontinuous derivatives" International Journal for Numerical Methods in Engineering **41**(7) 1215-1233.

P. Krysl and T. Belytschko (1999) "Element free Galerkin method for dynamic propagation of arbitrary 3-D cracks" International Journal for Numerical Methods in Engineering **44**(6) 767-800.

V. Lazarus, J.B. Leblond and S.E. Mouchrif (2001)"Crack front rotation and segmentation in mixed mode I+III or I+II+III. Part I: Calculation of stress intensity factors" Journal of Mechanical Physics and Solids **49**(7) 1399-1420.

J.M. Melenk and I. Babuška (1996) "The Partition of Unity Finite Element Method: Basic theory and applications" Computational Methods in Applied Mechanics and Engineering **39** 289-314.

N. Moës, J. Dolbow and T. Belytschko (1999) "A finite element method for crack growth without remeshing" International Journal for Numerical Methods in Engineering **46** 131-150.

N. Moës, A. Gravouil and T. Belytschko (2002) "Non-planar 3D crack growth by the extended finite element and level sets - Part I: Mechanical model" International Journal for Numerical Methods in Engineering **53**(11) 2549-2568.

J.T. Oden, C.A.M. Duarte and O.C. Zienkiewicz (1998) "New cloud-based hp finite element method" Computational Methods in Applied Mechanics and Engineering **153** 1117-126.

J. Oliver (1995)"Continuum modeling of strong discontinuities in solid mechanics using damage models" Computational Mechanics **17** 49-61.

J. Oliver (1996) "Modelling strong discontinuities in solid mechanics via strain softening constitutive equations. Part 2: Numerical Simulation" International Journal for Numerical Methods in Engineering **39** 3601-3623.

S. Osher and J.A. Sethian (1988) "Fronts propagating with curvature dependent speed: Algorithms based on Hamilton-Jacobi formulations" Journal of Computational Physics **79**(1) 12-49.

V.S. Rao, T.J.R. Hughes and K. Garikipati (2000)"On modelling thermal oxidation of Silicon II: numerical aspects" " International Journal for Numerical Methods in Engineering **47** 359-377.

M.M. Rashid (1998) "The arbitrary local mesh refinement method: An alternative to remeshing for crack propagation analysis" Computational Methods in Applied Mechanics and Engineering **154** 133-150.

M. Stolarska, D.L. Chopp, N. Moës, and T. Belytschko (2001) "Modeling crack growth by level sets in the extended finite element method" International Journal for Numerical Methods in Engineering **51** 943-960.

T. Strouboulis, I. Babuška and K. Copps (2000) "The design and analysis of the generalized finite element method" Computational Methods in Applied Mechanics and Engineering **181** 43-71.

T. Strouboulis, K. Copps and I. Babuška (2000) "The generalized finite element method: an example of its implementation and illustration of its performance" International Journal for Numerical Methods in Engineering **47**(8) 1401-1417.

N. Sukumar, D.L. Chopp, N. Moës and T. Belytschko (2001) "Modeling Holes and Inclusions by Level Sets in the Extended Finite Element Method" Computational Methods in Applied Mechanics and Engineering **190** 6183-6200.

N. Sukumar, N. Moës, T. Belytschko and B. Moran (2000) "Extended Finite Element Method for three-dimensional crack modeling" International Journal for Numerical Methods in Engineering **48**(1) 11549-1570.

Y. Sumi, C. Yang and Z.N. Wang (1996) "Morphological aspects of fatigue crack propagation .2. Effects of stress biaxiality and welding residual stress" International Journal of Fracture **82**(3) 221-235.

G. Ventura, J.X. Xu and T. Belytschko (2002) "A vector level set method and new discontinuity approximations for crack growth by EFG" International Journal for Numerical Methods in Engineering **54** 923-944.